

# Molecular Simulation of Shear Instabilities in Polyethylene and *n*-Alkane Crystals under Axial Compression

Mark R. McGann and Daniel J. Lacks\*

Department of Chemical Engineering, Tulane University, New Orleans, Louisiana 70118

Received April 2, 1998; Revised Manuscript Received June 1, 1998

**ABSTRACT:** Molecular simulations are used to elucidate compressive failure in polyethylene fibers. Compression of perfect polyethylene crystals is found to give rise to a long wavelength Euler buckling instability. The critical stress necessary to produce this buckling instability decreases as the wavelength of the instability increases, and it approaches the value of the lowest shear modulus in the limit of very long wavelength. The role of defects and the lamellar structure on the compressive failure mechanism of real polyethylene fibers is qualitatively addressed by simulations of *n*-alkane crystals. In contrast to the infinite chain systems, elastic instabilities in *n*-alkane crystals occur at stresses significantly below the lowest shear modulus; this reduction in the critical stress occurs because the instability allows the relaxation of intrachain distortions concentrated near chain ends which accumulate during compression. Similar elastic instabilities associated with defects and the lamellar structure in real polyethylene fibers could explain the experimental observation that the compressive strength of polyethylene is significantly lower than the measured shear modulus.

## 1. Introduction

Oriented polyethylene fibers and many other rigid-rod polymer fibers are significantly weaker in compression than in tension. The compressive failure in these polymer fibers has typically been attributed to a shear failure.<sup>1–6</sup> However, the specific molecular origin of this shear failure is unclear, due in part to the difficulty of carrying out experiments on the extremely narrow fibers. The present investigation uses molecular mechanics simulations to elucidate the compressive failure mechanism in polyethylene fibers.

Previous investigators have suggested that compressive failure is initiated through an elastic Euler buckling instability that occurs when the applied stress exceeds some critical stress ( $\sigma_c$ ).<sup>4</sup> This model approximates the polymer fiber as a collection of interacting parallel rods, with each rod corresponding to a single polymer chain (the diameter of each rod is thus  $\sim 5$  Å). An Euler buckling instability, shown schematically in Figure 1, arises from the competing responses of the potential energy and the stress–strain energy to the applied stress. Buckling corresponds to all chains bending into one of two symmetric buckled configurations (buckling of different chains in different directions is prohibited due to the high energy of such configurations). The potential energy, associated with both intrachain and interchain interactions, opposes buckling. In contrast, the stress–strain energy, associated with the axial length of the system, favors buckling. For a stress below  $\sigma_c$ , the potential energy contribution dominates, and thus the enthalpy (i.e., the sum of the potential energy and stress–strain energy) is a minimum for the straight chain configuration. However, as the stress exceeds  $\sigma_c$  the stress–strain energy dominates, and the enthalpy is a minimum for a buckled configuration; the straight chain configuration now corresponds to an enthalpy maximum rather than an enthalpy minimum (i.e., the second derivative in the direction of buckling is positive for stresses below  $\sigma_c$  and negative for stresses above  $\sigma_c$ ). For stresses greater than  $\sigma_c$ , the straight chain configuration is unstable and any infinitesimal displacement

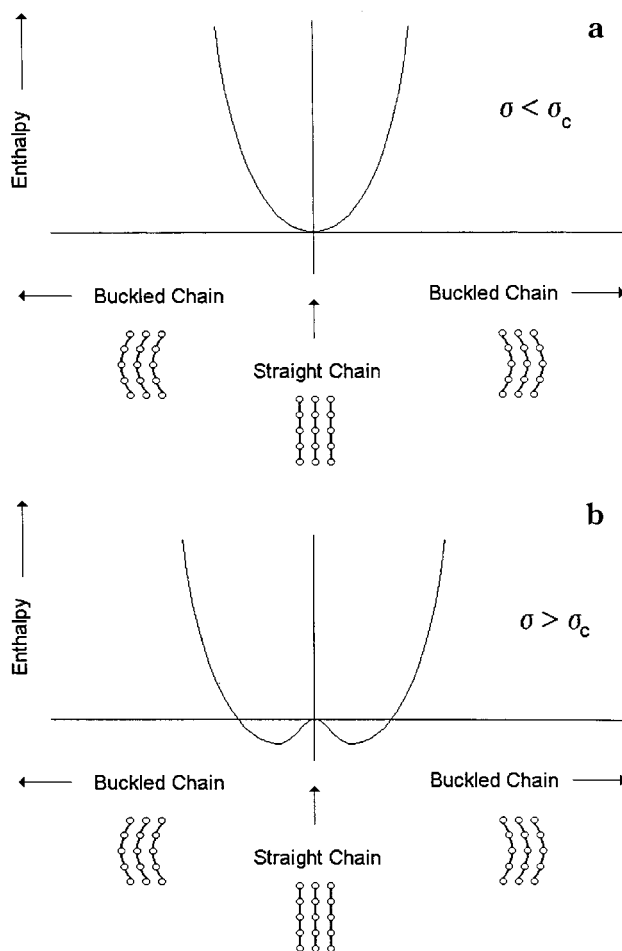


**Figure 1.** Enthalpy as a function of chain buckling: (a)  $\sigma < \sigma_c$ ; (b)  $\sigma > \sigma_c$ .

(e.g., from thermal motion) will result in the system buckling into one of the symmetric buckled configurations, with the particular configuration determined by the direction of this displacement.

A continuum model of Euler buckling<sup>4</sup> shows that the critical stress for an Euler buckling instability is given by

$$\sigma_c = \frac{C}{L^2} + G \quad (1)$$

where  $G$  is the shear modulus (due to the interchain interactions),  $C$  is a constant depending on the properties of a single chain, and  $L$  is the wavelength of the instability. While Euler buckling instabilities can occur with any wavelength, the longest wavelength Euler buckling instability occurs at the lowest stress and thus limits the material strength. In the limit of long wavelength, the intrachain contribution to eq 1 becomes negligible, and thus

$$\sigma_c = G \quad \text{for large } L \quad (2)$$

This continuum Euler buckling model thus finds that the compressive strength of a long chain system is equal to the shear modulus between chains.<sup>4</sup> Note that these results are independent of the diameter of the fiber (the relevant diameter in regard to buckling is the diameter of the individual polymer chains).

Several experimental studies have shown that the Euler buckling model predicts the compressive strength of polymer fibers to within 1 order of magnitude.<sup>1,7,8</sup> The Euler buckling model, however, overestimates the compressive strength in all cases. To explain these discrepancies with experiment, inelastic instabilities that precede the elastic Euler buckling instability have been proposed.<sup>1</sup> In the case of Kevlar, however, this discrepancy can be attributed to the difficulty of determining the relevant shear modulus from experiment.<sup>9</sup> Previous studies used the experimentally determined torsion modulus as the relevant shear modulus.<sup>1,7,8</sup> However, the torsion modulus represents an average of the shear moduli in different directions (due to a distribution of crystallite orientations), whereas Euler buckling is limited by the lowest shear modulus; the torsion modulus thus necessarily overestimates the relevant shear modulus. This problem is particularly acute for Kevlar, where the presence of hydrogen-bonded sheets causes the shear moduli in different directions to vary by over 1 order of magnitude.

The low compressive strength of polyethylene in relation to the torsion modulus cannot be rationalized in terms of crystallite orientations, because the failure stress is significantly lower than the smallest shear modulus. It has been proposed that defects and the lamellar structure in polyethylene fibers may cause the compressive strength to be lower than the shear modulus.<sup>7</sup> It is unclear, however, in terms of a molecular level interpretation, how the presence of defects or the lamellar structure affects the overall compressive strength of polymer fibers.

The present investigation uses molecular simulations to elucidate the compressive strength of polyethylene fibers. The qualitative effects of defects and the lamellar structure on the compressive strength are addressed by modeling *n*-alkane crystals. Previous molecular simulations of polymer fibers under compression have focused on intrachain conformational changes taking place over relatively short chain segments.<sup>10,11</sup> Euler buckling instabilities, however, occur over very long chain segments, causing interchain rather than intrachain interactions to dominate. These long wavelength

instabilities are difficult to model because they involve more atoms than can be practically modeled in a simulation cell. The present simulations thus use a computationally efficient Fourier space method to detect instabilities occurring over large length scales.

## 2. Computational Method

Molecular simulations are carried out that focus on elastic instabilities in perfect polyethylene and *n*-alkane crystals in the absence of thermal effects. The polyethylene simulations are based on infinite chain length molecules, and the *n*-alkane simulations focus on molecules with  $N = 13$  to  $N = 41$ , where  $N$  is the number of carbon atoms in the molecule. The force field of Karasawa et al. is used for the potential energy surface.<sup>12</sup> Ewald methods are used to evaluate the Coulombic and dispersion energy sums<sup>13</sup> for all systems, with the exception of simulation cells more than 50 Å in length. For these long systems the very elongated shape of the simulation cell severely impacts the efficiency of the Ewald method, and the Coulombic and dispersion energy sums are evaluated by direct space summations.

The unit cells of polyethylene and *n*-alkane crystals (with  $N$  odd) are orthorhombic and shown schematically in Figure 2. The unit cell of polyethylene crystals contains two chains with two repeat units along the chain axis. The unit cell of *n*-alkane crystals (with  $N$  odd) contains 4 molecules (two lamella with two *n*-alkane molecules per lamellae).<sup>14,15</sup> Note that only *n*-alkanes with  $N$  odd have crystal structures similar to that of polyethylene.

**2.1. Direct Space Simulations.** A direct space method is used to detect instabilities occurring within a single simulation cell (which may be composed of more than one unit cell). The crystal is initially allowed to relax to its zero pressure structure, by minimizing the potential energy with respect to the atomic coordinates and lattice parameters. Axial strain is then incrementally applied to the system by decreasing the  $c$  lattice parameter and then reminimizing the potential energy with respect to the atomic coordinates and remaining lattice parameters. The axial stress is determined at each strain from the first derivative of the energy with respect to the  $c$  lattice parameter, and an instability is detected by the presence of a maximum in the stress-strain curve.

The vibrational frequencies of the crystal, which are obtained by diagonalizing the second derivative matrix evaluated at the potential energy minimum, are measured as a function of stress. As the instability is approached, the curvature of the energy surface along one coordinate decreases toward zero (i.e., the second derivative along this coordinate is changing from positive to negative, see Figure 1), and thus the vibrational frequency associated with motion in this direction also decreases toward zero. The atomic displacements that lead to the instability are given by the eigenvector associated with the vibrational frequency that approaches zero.

**2.2. Fourier Space Simulations.** Instabilities that occur over more than one simulation cell are detected with a Fourier space method. This method analyzes vibrational frequencies of all wavelengths, for a system constrained to be in a straight chain configuration. The constraint is accomplished by including only one unit cell in the simulation cell, which precludes long-wavelength buckling.

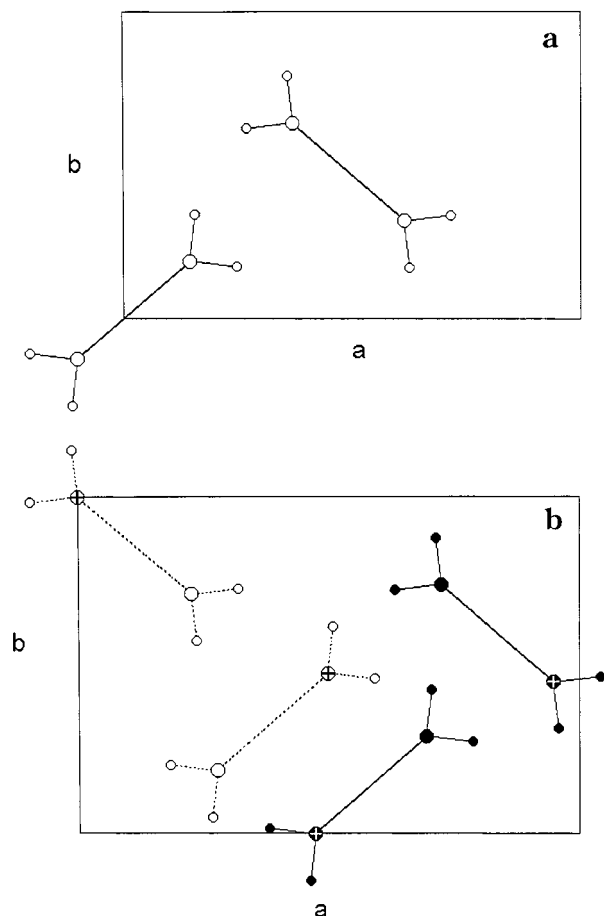


**Figure 2.** (a) Projection along the  $c$ -axis of the polyethylene unit cell. (b) Projection along the  $c$ -axis of an  $n$ -alkane unit cell with  $N$  odd. Large and small circles represent carbon atoms and hydrogen atoms, respectively. Atoms that line up when projected along the  $c$ -axis are shown as a single circle. For  $n$ -alkane crystals, chains with filled circles and solid lines are part of the upper lamella of the unit cell, chains with open circles and dashed lines are part of the lower lamella, and the plus symbol indicates the position of the starting and terminal carbon atoms.

As in the direct space method, the simulation cell (now consisting of only a single unit cell) is initially allowed to relax to its zero pressure structure, and strain is then incrementally applied to the system by decreasing the  $c$  lattice parameter and allowing the atomic coordinates and remaining lattice parameters to relax once again. The axial stress is again determined at each strain from the first derivative of energy with respect to the  $c$  lattice parameter.

An instability is now detected by observing vibrational frequencies decreasing to zero and becoming imaginary. The analysis of vibrational frequencies in Fourier space allows the inclusion of vibrational modes with any arbitrarily long wavelength<sup>16</sup> and thus allows the determination of buckling instabilities occurring over any arbitrarily long wavelength. This Fourier space method was used in our previous simulations of compressive instabilities in poly( $p$ -phenylene terephthalamide) crystals.<sup>9</sup>

It should be noted that the relaxation of the system to a potential energy minimum may seem to prohibit the existence of an imaginary frequency, which indicates that the crystal is at a potential energy saddlepoint rather than a potential energy minimum. The vibrations examined with the Fourier space method, however,

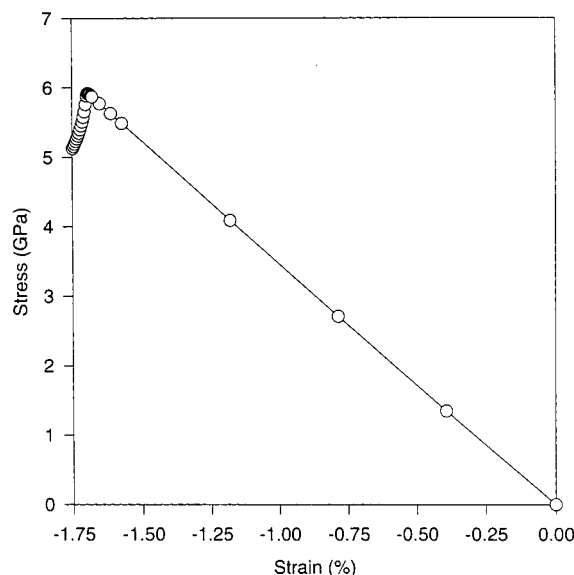


**Figure 3.** Stress vs strain curve for the polyethylene crystal with 10 unit cells comprising the simulation cell.

occur over many simulation cells, and the atomic displacements associated with these modes are prohibited during the relaxation step by the periodic boundary conditions. Modes with wavelengths less than the length of a single simulation cell that become unstable do cause the system to rearrange to a new energy minimum; detecting this shift to a new minimum is the basis of the direct space method.

### 3. Results and Discussion

**3.2. Polyethylene Crystals.** The stress-strain plot of the polyethylene crystal, with 10 unit cells explicitly modeled within the simulation cell (stacked along the chain axis), is shown in Figure 3. A buckling instability (which causes the chains to distort sinusoidally) occurs at the stress  $\sigma_c = 5.9$  GPa or strain  $\epsilon_c = -1.7\%$ , corresponding to the maximum in the stress-strain curve. Under constant strain conditions, the system remains stable as  $\epsilon_c$  is exceeded and buckling is reversed upon removal of the applied strain. Under constant stress conditions, however, once the applied stress exceeds  $\sigma_c$ , the system can no longer supply a stress equal to the applied stress, and the system continues to compress further until material failure occurs. This direct space simulation was repeated for simulation cells composed of 6 and 30 unit cells; the critical stresses obtained in these simulations are shown in Figure 4 (Note that the simulation with 6 unit cells per simulation cell corresponds to  $L = 7$  Å, and the simulation with 30 unit cells corresponds to  $L = 76$  Å).

The Fourier space method was also used to detect the critical stresses for instabilities with wavelengths of 6, 10, and 30 unit cells. The Fourier space and direct space methods yield identical results for these critical stresses, as shown in Figure 4. However, the computational cost of the Fourier space simulation is dramatically less than that of a direct space simulation. For example, detecting an instability occurring over 30 unit cells with the direct space method required approximately 5 days of CPU time. In contrast, detecting the same instability with the Fourier space method required 2 min of CPU time, which is a decrease in CPU time of more than 3 orders of magnitude. The Fourier space method was therefore used to determine the critical

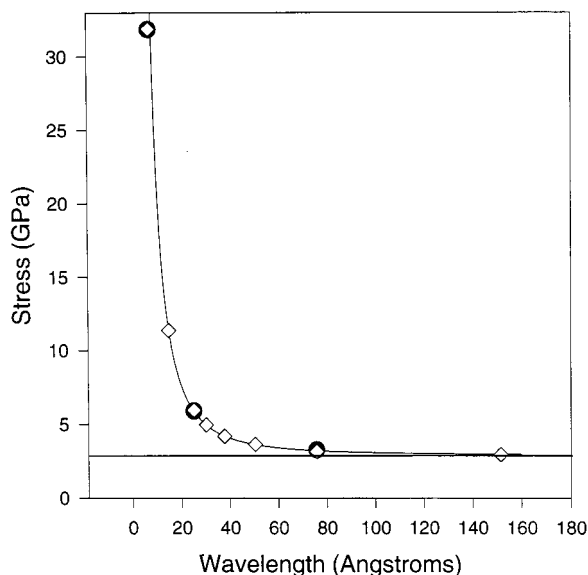


**Figure 4.** Critical axial stress that must be applied to produce an instability in the polyethylene crystal vs the wavelength of the instability. Open diamonds are Fourier space results and filled circles are direct space results. The curve is a fit of the present results to the Euler buckling model proposed by DeTeresa et al.<sup>4</sup> (eq 1). The horizontal line is the shear modulus in the *bc* plane of the unstressed crystal.

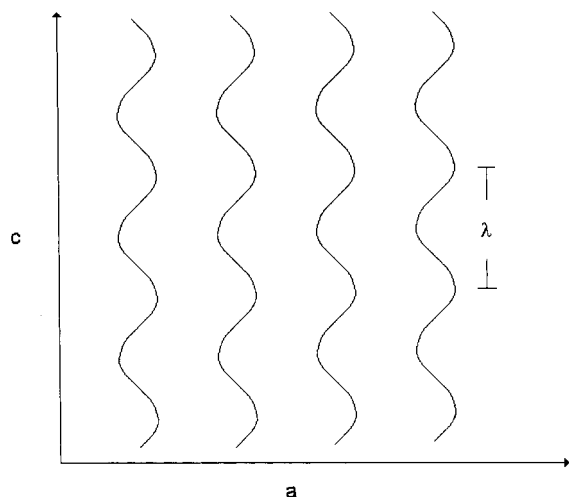


**Figure 5.** Schematic of the transverse acoustic vibrational modes that propagate along the chain axis. The wavelength of the vibration is  $\lambda$ .

stress for other wavelengths of the instability, and these results are shown in Figure 4.

In all cases the vibrational mode associated with the instability is the transverse acoustic mode (shown schematically in Figure 5); these atomic displacements correspond exactly to the Euler buckling mechanism proposed by DeTeresa et al.<sup>4,7</sup> The present simulation results for the critical stress as a function of wavelength follow a functional relationship of the form predicted by the continuum Euler buckling model (eq 1). The fit of eq 1 to the simulation results shown in Figure 4 yields  $G = 2.84$  GPa, which is slightly lower than the shear modulus in the *bc* plane directly calculated from the appropriate second derivative of the potential energy for the unstressed crystal (2.97 GPa). The shear modulus, however, is a slight function of applied stress, and at incipient instability the shear modulus was directly calculated to be 2.84 GPa, which matches

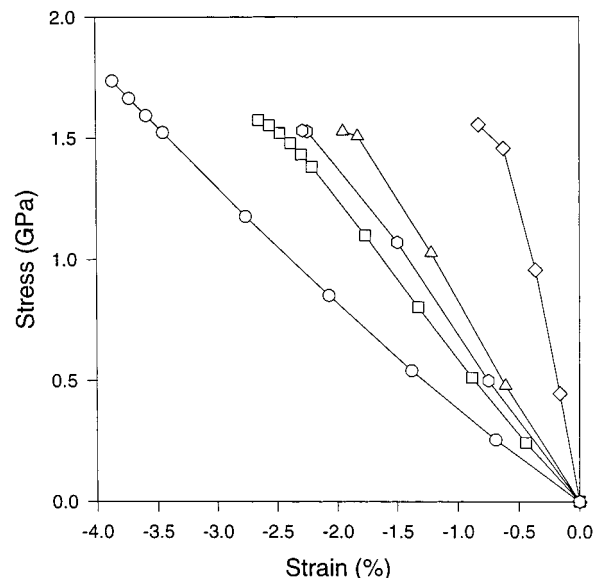


**Figure 6.** Stress-strain curves for the *n*-alkane systems. Circles, squares, hexagons, triangles, and diamonds represent the systems with 13, 21, 25, 31, and 41 carbon atoms per chain, respectively.

exactly the modulus predicted by the fit to eq 1. We conclude therefore that Euler buckling instabilities occur in these simulations of perfect polyethylene crystals.

**3.2. *n*-Alkane Crystals.** Vibrational frequencies of modes extending over many unit cells were examined with the Fourier space method as a function of compressive stress for *n*-alkane crystals. Vibrational modes extending over more than one unit cell in the *a* and *b* directions, in addition to the *c* direction, were analyzed. However, it was found that the instabilities occurring at the lowest stress were associated with distortions confined to one unit cell (in contrast to polyethylene).

Stress-strain curves for *n*-alkane crystals are shown in Figure 6, and the critical stresses necessary to produce instabilities in these crystals are shown in Figure 7. Instabilities in these systems occur at stresses significantly lower than the shear modulus of the system ( $G \sim 2.8$  GPa for these *n*-alkanes). The eigenvector associated with the vibrational mode that becomes unstable indicates that the instability proceeds through a "chain tilting" displacement, shown schematically in Figure 8. Thus the instabilities in *n*-alkane systems occur below the shear modulus, by an elastic mechanism distinct from Euler buckling.

To understand why the instabilities occur at stresses less than the shear modulus, the relative contributions of the intrachain and interchain contributions to the curvature of the potential energy surface in the direction of the instability are examined. Interchain interactions (associated with shearing between neighboring chains) are found to oppose the instability (i.e., the curvature due to interchain interactions is positive) in both *n*-alkane and polyethylene crystals. Intrachain interactions (associated with torsions and angle bending) in polyethylene crystals are also found to oppose the instability (although this contribution becomes negligible for long wavelength instabilities). In contrast, intrachain interactions in *n*-alkane crystals are found to favor the instabilities (i.e., the curvature due to intrachain interactions in *n*-alkane crystals is negative) and act to reduce the critical stress of the system.



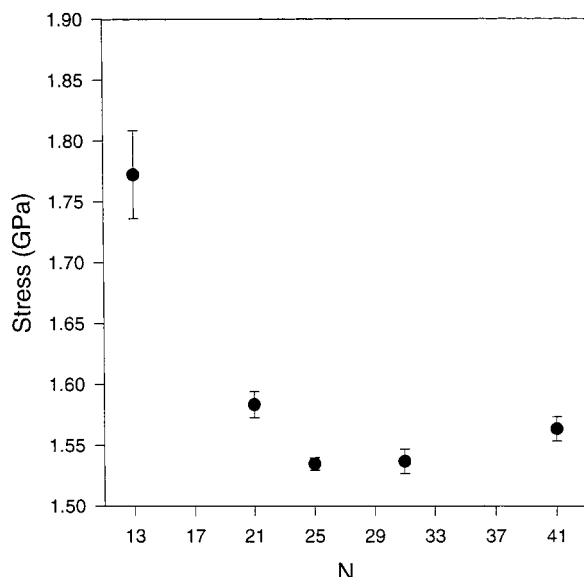


**Figure 7.** Critical stress required to produce instabilities in *n*-alkane crystals as a function of the number of carbon atoms per chain.

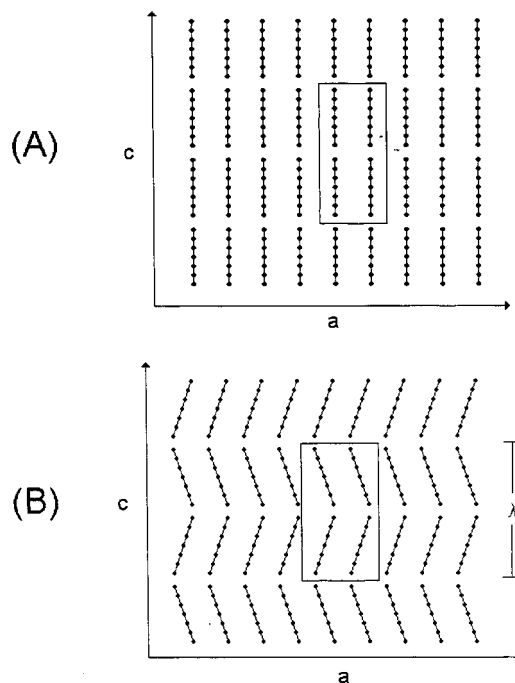


**Figure 8.** Schematic of an undistorted *n*-alkane crystal (A) and the configuration associated with the "chain tilting" instabilities (B). Each line represents a single chain, each circle represents a methyl or methylene group, the box denotes the unit cell, and the wavelength of the vibrational mode is  $\lambda$ .

The reason intrachain interactions in *n*-alkane crystals favor the instability has been examined. The packing interactions between axially neighboring chains leads to some distortion within the chains relative to the free chain configuration; these distortions are concentrated near the chain ends because methyl groups have more difficulty packing in the lamellae than methylene groups. As the crystal is compressed, these intrachain distortions increase in magnitude. However, the chain tilting instability reduces axial packing interactions, which allows the chains to relax to less distorted (lower energy) configurations. For longer chain lengths ( $N > 25$ ), the intrachain distortions

become less significant as the chain length is increased, because the distortions are concentrated near the chain ends and the chain ends represent a decreasing fraction of the total chain. The critical stress therefore increases with increasing chain length in the long chain regime, as seen in Figure 7 and will eventually converge with the result for perfect polyethylene crystals as the chain length becomes very large. For shorter chain lengths ( $N < 25$ ), the distortions become more significant as the chain length is increased, because for these short chains the distortions encompass the entire chain length; the critical stress therefore decreases with increasing chain length in the short chain length regime, as seen in Figure 7.

The present results suggest that the defects and lamellar structure that exist in real polyethylene fibers can lower the compressive strength to significantly below the shear modulus, in that intrachain distortions which favor instabilities will accumulate near defects (such as a chain end within a lamellae) and lamellar surfaces as the fiber is compressed. The continuum Euler buckling model assumes that all potential energy interactions act to increase the compressive strength of the fiber and thus does not include this effect.

#### 4. Conclusion

The present molecular simulations find that long wavelength Euler buckling instabilities occur as perfectly crystalline polyethylene is compressed, as previously suggested with a continuum model by DeTeresa et al.<sup>4</sup> The critical stress required to produce the Euler buckling instabilities in infinite polymer chain systems decreases as the wavelength of the instability increases and approaches the value of the lowest shear modulus in the limit of long wavelength.

In contrast, a different type of elastic instability takes place as *n*-alkane crystals are compressed, which occurs at stresses significantly below the lowest shear modulus. The instabilities in *n*-alkane crystals have wavelengths equal to the length of a single unit cell and correspond to the chains in a given lamellae tilting away from the direction of the applied stress. Such tilting displacements allow the relaxation of intrachain distortions concentrated at chain ends, which are caused by compression.

We propose that the compressive behavior of real polyethylene fibers will be somewhat similar to that found in the present simulations of *n*-alkane crystals; i.e., elastic instabilities will occur that allow the relaxation of intrachain distortions concentrated at defects and lamellar surfaces and caused by compression. This mechanism can explain the experimental observation that the compressive strength in polyethylene fibers is significantly less than the shear modulus.

**Acknowledgment.** Funding from the National Science Foundation (grant number DMR-9624808), the Louisiana Board of Regents, and the donors of the Petroleum Research Fund as administered by the American Chemical Society is gratefully acknowledged.

#### References and Notes

- (1) Vlattas, C.; Galiotis, C. *Polymer* **1994**, *35*, 2335.
- (2) Takahashi, T.; Miura, M.; Sakurai, K. *J. Appl. Polym. Sci.* **1983**, *28*, 579.
- (3) Martin, D. C.; Thomas, E. L. *J. Mater. Sci.* **1991**, *26*, 5171.
- (4) DeTeresa, S.; Porter, R.; Farris, R. *J. Mater. Sci.* **1985**, *20*, 1645.

- (5) Shigematsu, K.; Imada, K.; Takayanagi, M. *J. Polym. Sci.* **1975**, *13*, 73.
- (6) Robertson, R. E. *J. Polym. Sci.* **1969**, *7*, 1315.
- (7) DeTeresa, S. J.; Porter, R. S.; Farris, R. J. *J. Mater. Sci.* **1988**, *23*, 1886.
- (8) Mehta, V.; Kumar, S. *J. Mater. Sci.* **1994**, *29*, 3658.
- (9) Lacks, D. J. *J. Mater. Sci.* **1996**, *31*, 5885.
- (10) Wierschke, S. G.; Shoemaker, J. R.; Haaland, P. D.; Patcher, R.; Adams, W. W. *Polymer* **1992**, *33*, 3356.
- (11) Klunzinger, P. E.; Eby, R. K. *Polymer* **1993**, *34*, 2431.
- (12) Karasawa, N.; Dasgupta, S.; Goddard, W. A. *J. Phys. Chem.* **1991**, *95*, 2260.
- (13) Karasawa, N.; Goddard, W. A. *J. Phys. Chem.* **1989**, *93*, 7320.
- (14) Norman, N.; Mathisen, H. *Acta Chem. Scand.* **1972**, *26*, 3913.
- (15) Smith, A. *J. Chem. Phys.* **1953**, *21*, 2229.
- (16) Ashcroft, N. W.; Mermin, N. D. *Solid State Physics*; Saunders College Press: Philadelphia, 1976.

MA9805203